The Monte Carlo Method: Versatility Unbounded In A Dynamic Computing World
Chattanooga, Tennessee, April 17–21, 2005, on CD-ROM, American Nuclear Society, LaGrange Park, IL (2005)

THE APPLICATIONS OF MONTE CARLO CODES TO ROMANIAN TRIGA AND CANDU REACTORS

E.D. Gugiu, R.J. Ellis[*] and Cs. Roth
Institute for Nuclear Research (INR)
PO Box 78, Pitesti, 0300, Romania
danagugiu@yahoo.com; ellisrj@ornl.gov; croth@scn.ro

ABSTRACT

The aim of the paper is the presentation of the results obtained using the MCNP5, MCNP-X, MONTEBURNS1.0 and SCALE 4.4a codes in various projects related to TRIGA and CANDU reactors: the set up of the ΣΣ system (secondary intermediate–energy standard neutron field) in the thermal column of the steady-state core of the Romanian TRIGA, neutron dosimetry, the computations of some parameters related to different CANDU fuel bundle concepts, and the replacement of the original stainless steel adjuster rods by cobalt rods in CANDU reactor core. The analysis of the results obtained and a discussion regarding nuclear data needs are presented.

Key Words: Monte Carlo, reactors

1 INTRODUCTION

As proved during the years, the Monte Carlo method is the most appropriate and suitable method to simulate complex 3-D geometries, and to solve the complex problems involving statistical processes such as the interaction of radiation with materials. Therefore, Monte Carlo codes are mostly used in the specific works related to Romanian TRIGA and CANDU reactors.

The TRIGA-INR facility has two reactors in the same pool: the 14-MW TRIGA-INR SSR (steady-state reactor) and a 500 kW (pulse to 20 GW) ACPR (annular core pulsing reactor). The 14-MW TRIGA, originally HEU fueled, is undergoing full conversion to LEU fuel, facilitated by a DOE nonproliferation initiative in which the U.S. is funding an agreement where CERCA (Framatome/AREVA & Siemens) supplies fresh LEU fuel, through a contract with IAEA. The CANDU-6 is a 700-MW_{th} pressurized heavy water reactor design, using natural uranium oxide fuel. Romania currently has two CANDU-6 NPPs: Cernavoda-1, in operation since 1996, and Cernavoda-2, which is in the final stages of construction.

The set up of the thermal neutron flux cavity and of the ΣΣ reference spectrum system in the TRIGA thermal column are based on the preliminary simulations performed using MCNP-5 [1] and KENO codes [2]. Also, the codes were used in the next stages related to the aspects regarding the improvement of the spectral characteristics of these thermal and epithermal neutron irradiation facilities. An analysis of the computational results and measurements is presented.

In the work concerning the Bonner type spectroscopy method, MCNP 5 and MCNP-X [3] have been used in order to evaluate the response matrix of the detector and to simulate the complex geometries related to the experimental measurements.

---

[*] **Oak Ridge National Laboratory, P.O. Box 2008, Oak Ridge, Tennessee, USA 37831-6172**

MCNP 5, MONTEBURNS 1.0 [4] and ORIGEN-ARP 2.00 [5] are used in computational work related to various CANDU fuel type projects to evaluate some local parameters (k-infinity values, void coefficient of reactivity, pin power factors) and to analyze the influence of different neutron cross-section libraries on the parameter values. The computations are performed for fresh fuel and for various burn-up points, for actual, detailed geometries and material compositions of the fuel bundles.

In the work concerning ^{60}Co production in CANDU reactors, the analysis of neutronic and thermalhydraulic aspects related to the cobalt adjuster rods (cobalt mass evaluations, cobalt burn-up, the impact on CANDU core reactivity and evaluation of the dose and heating of the cobalt adjuster rods) is performed using MCNP5 and MONTEBURNS 1.0, as well as ORIGEN2.1 [6] as a stand-alone code. The analysis of the results obtained and comments regarding nuclear data are also presented in the paper.

2 EXPERIMENTAL DEVICES AT TRIGA REACTOR THERMAL COLUMN

The TRIGA reactor thermal column is a graphite block formed by 98 rectangular graphite cells in aluminum cladding positioned into the reactor pool on the north side of the active core.

2.1 Thermal Flux Cavity Characterization

A thermal flux irradiation facility was created in the thermal column by replacing 36 central bricks with a graphite block having a spherical central cavity. A dry channel (8 m high) was developed on the top of the thermal flux cavity for access and instrumentation purposes. The device is designed so that it allows the placement of the ΣΣ standard system and of the fission chambers afferent instrumentation into the cavity. In order to check up the level of the flux in the cavity, an additional monitoring system (besides the reactor control system) is needed. It consists in two sealed fission chambers placed in the thermal column, in dry channels, which allows the opportunity to obtain local information regarding the neutron flux density in the cavity.

In the first stages of the device implementation, preliminary estimations of the flux-spectrum in the central cavity, as well as characterization of the flux monitor locations have been performed using MCNP-4C for the actual, detailed geometry and material composition of the device. In these early steps the active core was not simulated, but a surface neutron source was considered on the side wall from the core (based on the flux and flux distribution measurements). Two other types of neutron source, more or less probable, were also considered in the simulations: a uniform source distribution on the surface, and a linear increasing source in the horizontal direction. The aim of the computations performed for all the available monitor locations (codified in Fig.1) is to identify the positions where the ratio between the flux in the respective location and the flux in the central cavity is nearly independent of the source distribution.

The results are presented in Fig.2, Fig.3 and Fig.4.

Analyzing the values obtained for the three types of sources (distributed source – series 1, uniform source – series 2 and linear source – series 3) one can say that the type J locations are influenced by the source distribution; instead, positions like B2, B6, C2, C3, C6 and C7 could be recommended as monitor locations.

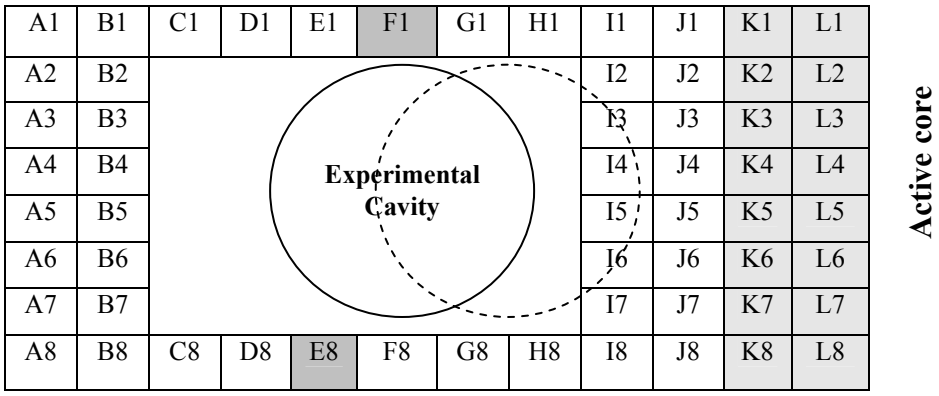

Figure 1. TRIGA Thermal column codification

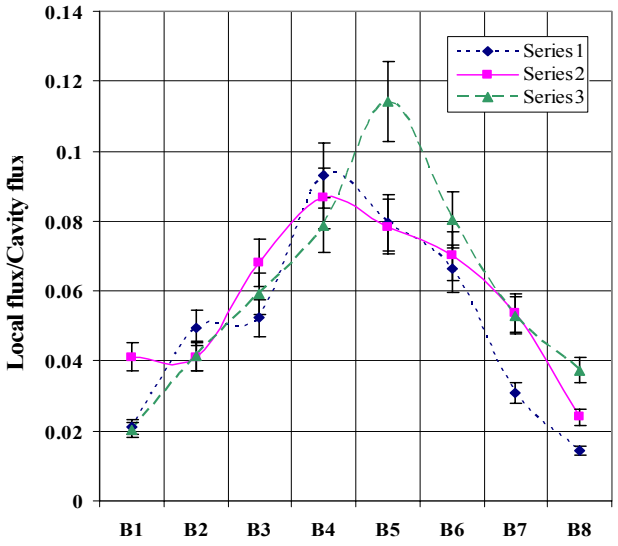

Figure 2. Flux distribution in locations B

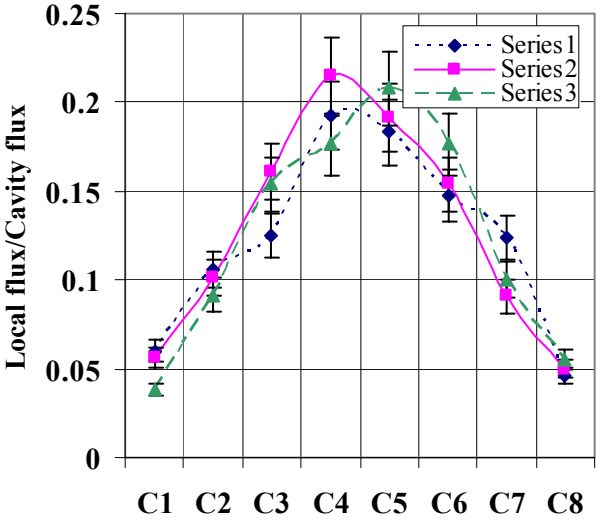

Figure 3. Flux distribution in locations C

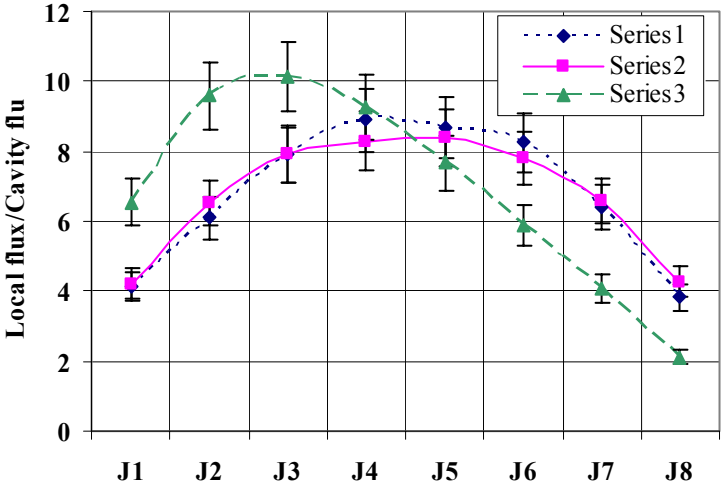

Figure 4. Flux distribution in locations J

Measurements using fission chambers and foil activation technique have been also performed in this first stage of the thermal column characterization in order to estimate the flux and the flux spectrum in the central cavity. The results of the measurements show a significant epithermal contribution (around 10%) and a cadmium ratio for gold below 20.

Thus new MCNP-4C computations have been done for various configurations of the column in order to find out the solutions for improving the cavity spectral characteristics. This time, the simulations (using KCODE option) were performed taking into account the detailed geometry and composition of the TRIGA active core; also, a water layer of 2 mm was considered between the graphite bricks of the column (due to some geometry and positioning imperfections). Analyzing the results, we decided to move the central cavity away from the active core (Fig. 1-doted line) with one row of graphite bricks (14.3 cm). The MCNP-4C flux distributions along the three axes also have been simulated (Fig.5).

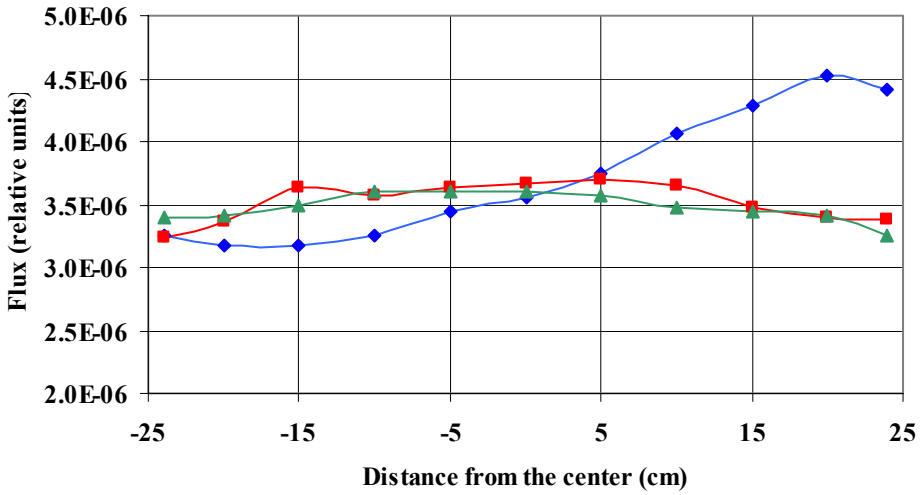

Figure 5. Flux distributions - MCNP-4C results

The measurements of the flux distributions performed using a special device instrumented with Mn 80.2% -Cu wires show a very good agreement with the computations (Fig.6). The discrepancies observed along the last 5 cm are due to the stopper hole which was not considered in the MCNP simulations.

The measured fission and activation reaction rates are processed by SAND-II code using the MCNP computed spectrum as guess spectral shape in order to perform the spectrum unfolding from the experimental data. The solution spectrum is obtained after 4 iterations with a standard deviation between the measured and computed activities bellow 4%.

The Monte Carlo computations, as well as the measurements performed show improved characteristics of the thermal column in the new configuration (a cadmium ratio for gold greater than 60.0 and a reduced contribution of the epithermal neutrons: 1.7%). Even in this case, the epithermal component is a little larger by comparison to the reference spectra and it is mainly due to the smaller dimensions of our column and to the water layer (2 mm) existing among the graphite cells.

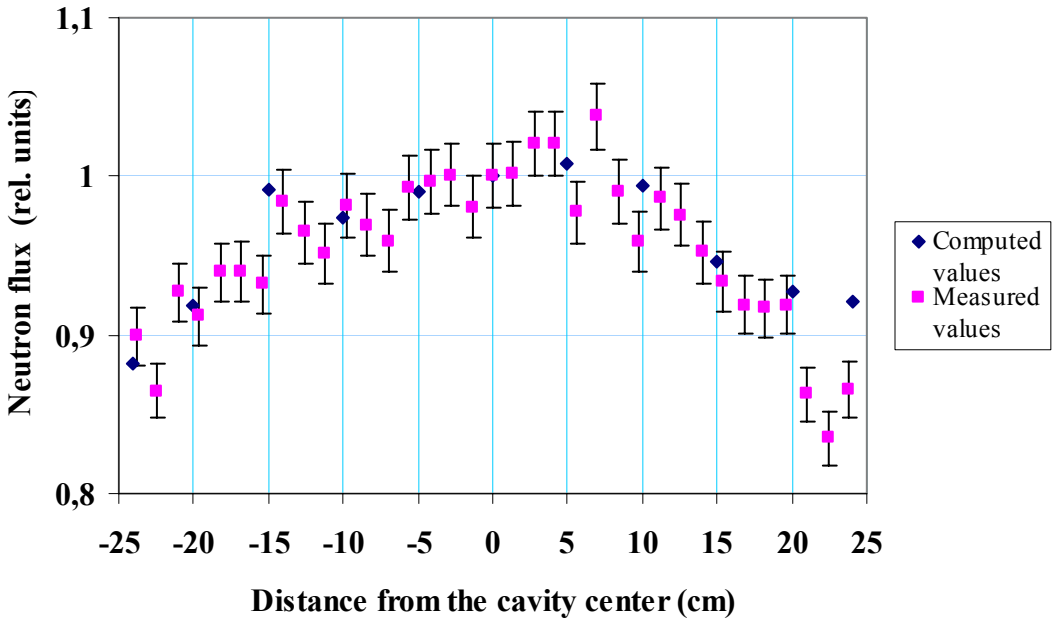

Figure 6. Flux distribution comparison

One may conclude that the agreement between the experimental and computed results proved that the Monte Carlo method is well suited for these types of experiments.

2.2 The ΣΣ Irradiation Facility

ΣΣ is a thermal-fast coupled spherical assembly positioned into the thermal flux cavity. The spherical natural uranium shell surrounds an aluminum-clad spherical shell of natural boron; the diameter of the central hole is of 11 cm. MCNP-4C code was used in the simulations performed in order to characterize the ΣΣ reference spectrum. The detailed, actual geometries of the thermal column and of the TRIGA reactor core were considered in the computations; the only simplification is regarding the reactor fuel which was homogenized for each bundle. The MCNP-4C computed spectrum is compared with the ΣΣ-ITN spectrum [8] and with the recommended ΣΣ spectrum [9] (Fig.7).

Measurements using foil activation techniques and fission chambers followed by a spectrum unfolding procedure have been also performed [10]. The recommended ΣΣ spectrum, as well as the MCNP-4C computed spectrum has been used as guess spectra for unfolding. The convergence is faster in the latter case and the standard deviations of the computed reaction rate relative to the measured ones are smaller than 3.5% (Tab. I).The unfolding computations performed using SAND - II code show that the MCNP-4C computed spectrum is the best option as guess spectrum.

The average energy of the ΣΣ spectrum (0.846 MeV) was also computed using MCNP code; it is greater than that of some reference spectra, 0.783 MeV [8] or 0.827 MeV [9], because

of the larger fast component of the spectrum due to the smaller dimensions of the thermal column.

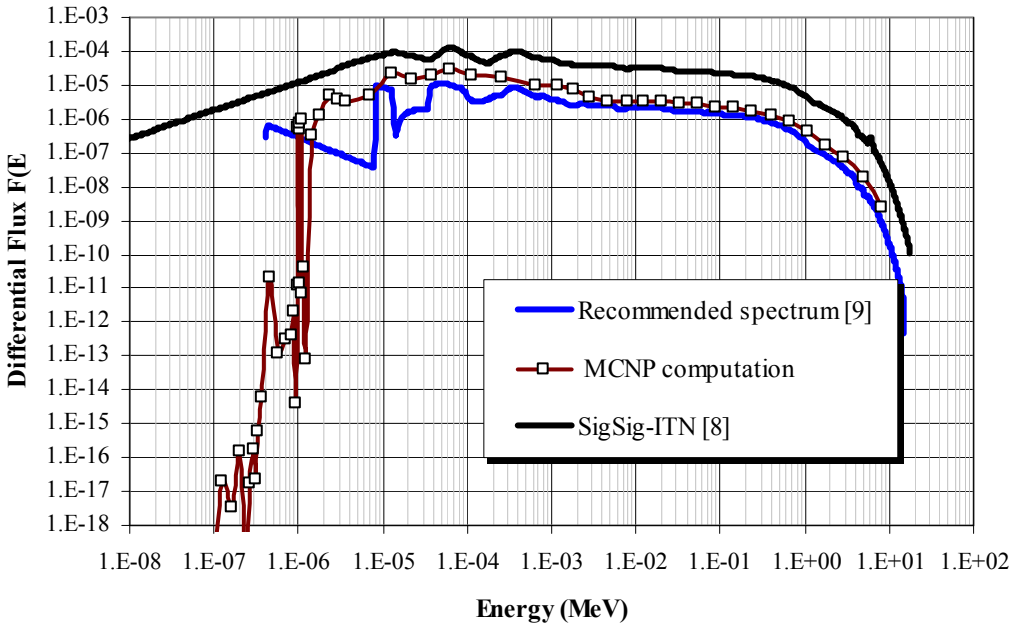

Figure 7. Sigma-Sigma spectrum computation results

Table I. Comparison of the measured and computed reaction rates

Reaction	Reaction rate		Energy response range		Deviation (%)
	Measured (cps)	Computed (cps)	E_{low} (MeV)	E_{high}(MeV)	
$^{27}Al(n,\alpha)$	$1.060\ 10^{-21}$	$1.066\ 10^{-21}$	6.5	12.1	-0.61
$^{235}U(n,f)$	$9.120\ 10^{-18}$	$9{,}221\ 10^{-18}$	$2.1\ 10^{-4}$	2.8	-1.10
$^{238}U(n,f)$	$5.589\ 10^{-19}$	$5.737\ 10^{-19}$	1.4	6.3	-2.58
$^{237}Np(n,f)$	$3.743\ 10^{-18}$	$3.933\ 10^{-18}$	$4.\ 5\ 10^{-1}$	4.5	-4.83
$^{239}Pu(n,f)$	$1.054\ 10^{-17}$	$1.060\ 10^{-17}$	$2.0\ 10^{-4}$	3.2	-0.53
$^{197}Au(n,\gamma)$	$2.550\ 10^{-18}$	$2.508\ 10^{-18}$	$5.\ 0\ 10^{-6}$	$7.2\ 10^{-1}$	+1.68
$^{115}In(n,n')$	$4.000\ 10^{-19}$	$3.805\ 10^{-19}$	$9.2\ 10^{-1}$	5.4	+5.14
$^{58}Ni(n,p)$	$1.770\ 10^{-19}$	$1.721\ 10^{-19}$	1.8	7.4	+2.82
Standard deviation of the measured and computed reaction rates:					3.14 %

In conclusion, the Monte Carlo method is the most suitable for a detailed neutron characterization of these facilities. The computations and the experimental work have been performed in order to achieve and to substantiate the documentation required for these facilities accreditation.

3 BONNER TYPE SPECTROMETRY

The development of the Bonner spectroscopic method based on the use of a high sensitivity thermal neutron detector (BF_3 cylindrical proportional counter, type RS-P1-1613), supplied by REUTER STOKES and, 10 various thickness cylindrical high density polyethylene shielding is presented in the following. MCNP4C code is used to simulate the actual geometry of the detector and to evaluate the response functions for each shielding thickness and for the bare detector for energies between 10^{-10} MeV and 18 MeV, corresponding to the SAND II unfolding code energy mesh limits. The spectrometer response is computed for isotropic neutron flux and reported to the unperturbed flux in the detector position. The response functions for 10 polyethylene thicknesses are presented in Fig.8.

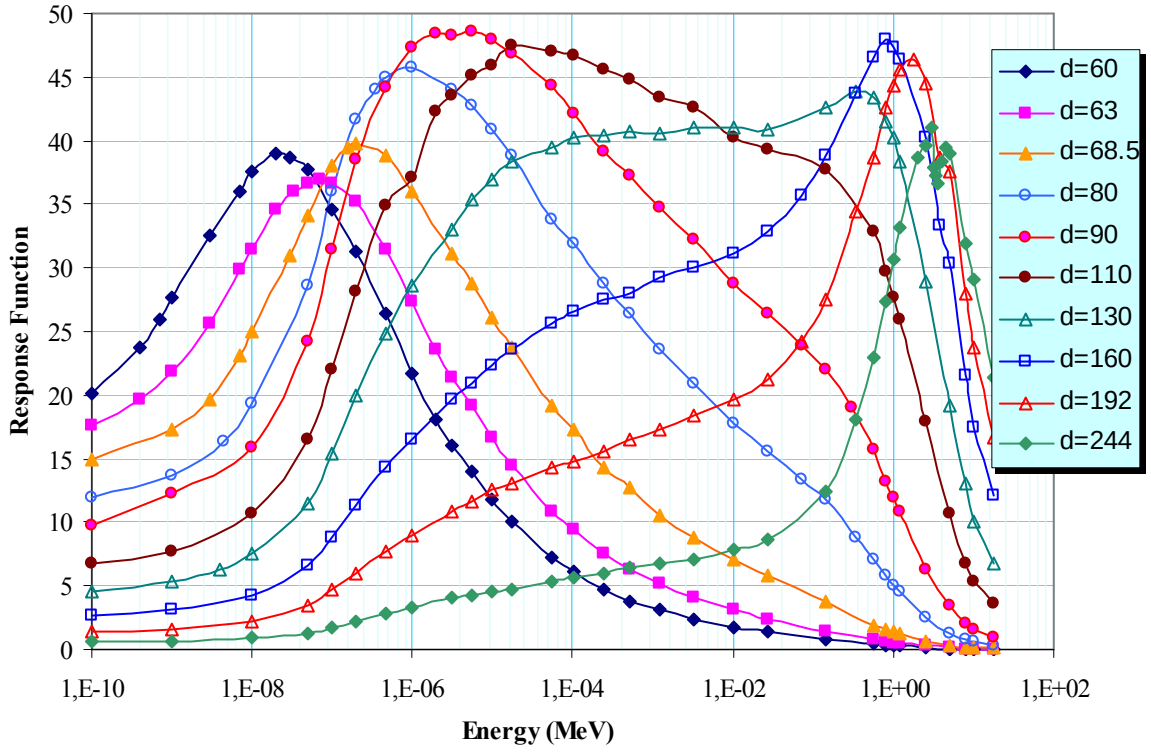

Figure 8. Response functions

The response functions cover the entire energy range, beginning from thermal energies up to a few MeV. The intermediate energies are well covered by 110 mm and 130 mm diameter polyethylene shielding. For higher energies (E>14 MeV), additional shielding, with larger thicknesses, are required. This is necessary only for some special cases (e.g. dosimetry for exposure to cosmic radiation). In the most experimental situations (nuclear reactors, radionuclide neutron sources) the neutron energy limit of 14 MeV is an acceptable approximation. Lin-log interpolation between computed values, followed by numerical smoothing is used to generate the response matrix in SAND II energy grid (621 points).

The disadvantage of the cylindrical spectrometer is due to the fact that the response function is affected by its position in the anisotropic neutron field. Therefore, some evaluations and considerations related to the anisotropy effects and the circumstances under which the device could be used are presented. Computations using MCNP-X are performed for two case types: indoor measurements (room of various dimensions) and outdoor measurements (neutrons from the cosmic rays).

In the first case, simulations are performed for two polyethylene thicknesses (4.5 and 70.5 mm) and for room dimensions of 2x2x2, 4x4x4 and, 6x6x6 m respectively. The source is located in the center of the room (maximum sensitivity position). The unperturbed response functions (infinite medium) are computed for the same geometries of the detector-source assemblies. Some results are presented in Fig.9 and Fig.10.

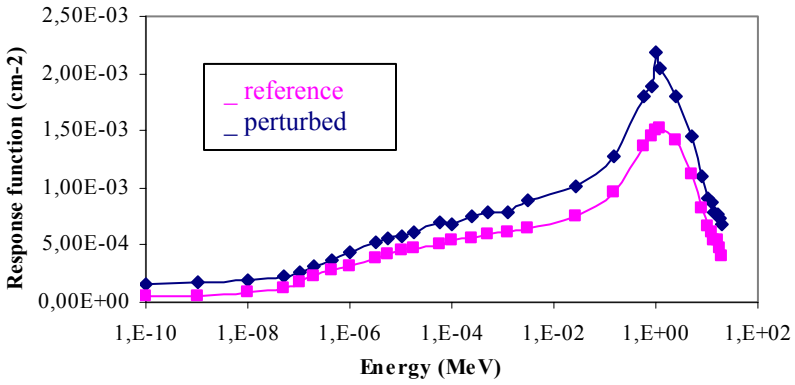

Figure 9. Detector with 70.5 mm shielding

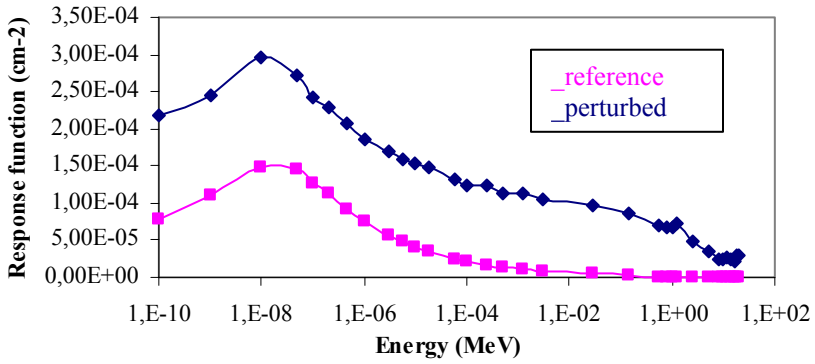

Figure 10. Detector with 4.5 mm shielding

Analyzing all the results, one can observe that the perturbed response functions have the same patterns as the unperturbed ones, but the values are significantly increased. Also, the

increasing of the perturbed values is greater around 1 MeV and is due to the resonances in the concrete scattering cross-section. It is obvious that the presence of other "objects" in the room will increase the anisotropy of the neutron field. Therefore, the use of this spectrometer type implies the use of an appropriate response matrix that should take into account the anisotropy by a proper simulation of the source. A solution of this problem could be achieved by locating the detector in a maximum sensitivity position (obtained by previous simulations and measurements) which will overestimate the dose (up to 30%), but it is a time consuming method and less efficient.

In outdoor experiments one can find out a detector position which is not affected by the scattered neutrons. The response matrix is generated for a plane isotropic source and for horizontal detector position. Simulations are also performed in order to set up the distance from the soil or concrete at which the contribution of scattered neutrons is negligible. Computations have been done for various polyethylene thicknesses and for different distances and soil compositions (some results are presented in Fig.11).

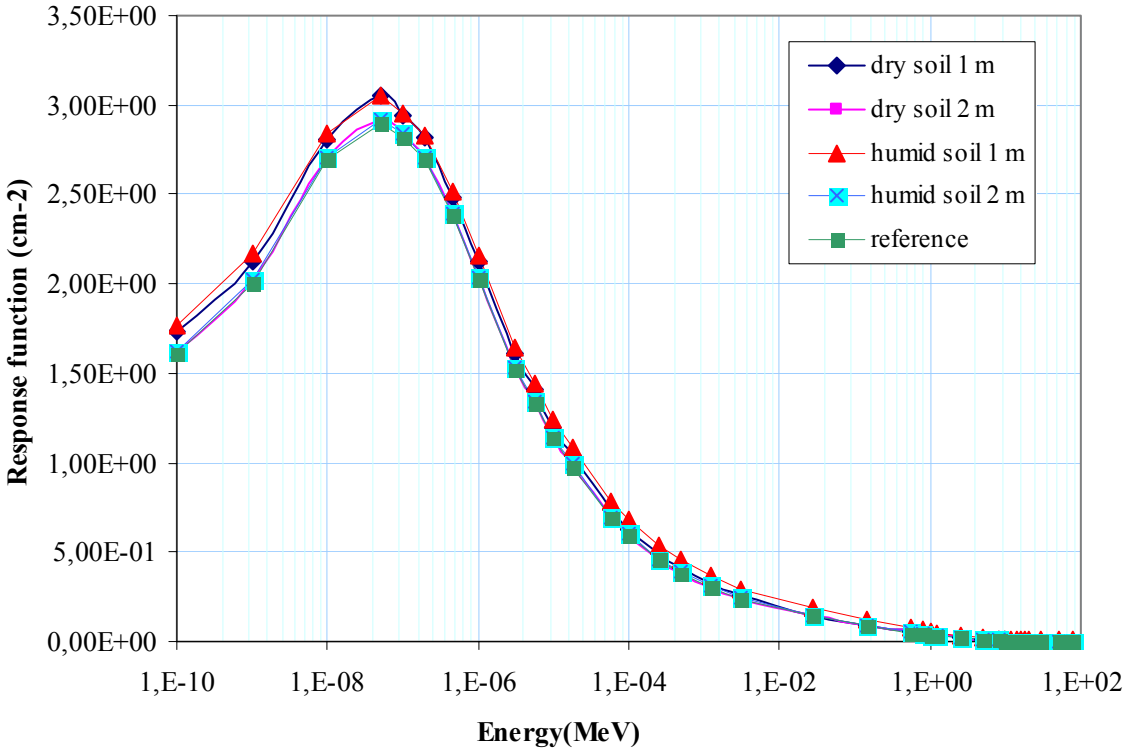

Figure 11. Detector with 4.5 mm thickness shielding at various distances and soil types

The computed response function (Fig.11) is slightly perturbed at 1 m and is almost identical at 2 m distance with the reference one (infinite medium). There are not differences between dry and humid soil simulation results. The same conclusion is carried out by the computations performed for concrete. As a result, at distances greater than 2 m from the soil the

scattered neutron contribution is negligible and the spectrometer can be used to monitor the natural radiation background.

4 CANDU FUEL TYPE PROJECTS

Because of their capabilities, MCNP 5 and MONTEBURNS 1.0 codes were used in order to asses the accuracy of some local parameters computed for CANDU type fuels using probabilistic and deterministic codes. The simulations are focused on the evaluations of the k-infinity eigenvalues and absolute void reactivity values defined as:

$$\rho = \left(1/k_{ref} - 1/k_{void}\right)\times 1000 \quad \text{(mk)} \qquad (1)$$

where: k_{ref} is the k-infinity value for the reference state (normal coolant operating state), and k_{void} is the k-infinity for the specified void fraction (0, 25, 50, 75 and 100%). The void fraction is related to the loss of coolant accident (LOC) and represents the coolant density changes.

The computations are performed for standard CANDU bundle (37 fuel pins) and for SEU-43 (Slightly Enriched Uranium) cell (43 fuel pins – Fig.12) for fresh fuel as well as for various burn-up points. All the Monte Carlo runs are done for the actual, detailed 3 D geometries of the bundles; the starting neutron source has a uniform volume distribution in all the fuel rods and is generated from a Watt spectrum.

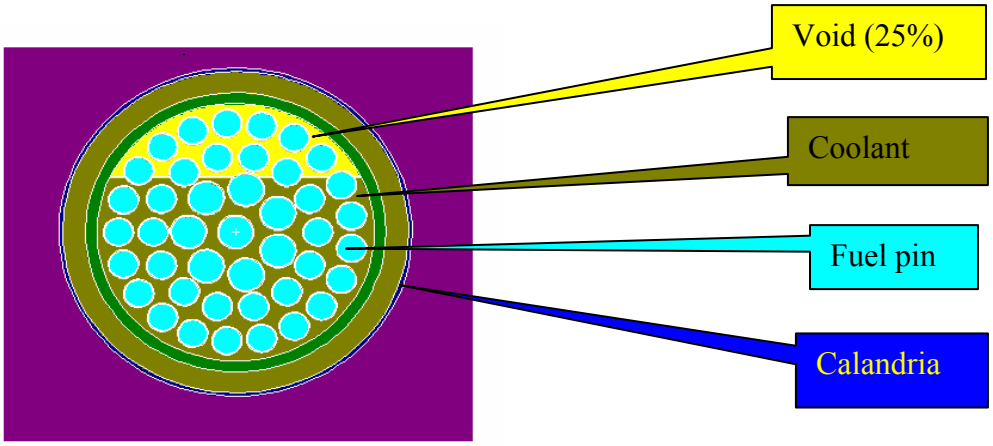

Figure 12 CANDU- SEU fuel bundle

For CANDU standard, a homogenized model of the coolant is considered (decreasing values of the coolant density during LOC). The void reactivity values for fresh fuel computed with CP_2D code [7] plus WIMSD5B library and MCNP 5 plus ENDF/B VI library show the same behavior with the coolant densities; the differences are due to the distinct mathematical models and neutron cross-section libraries (Fig.13).

Burn-up computations are performed using MONTEBURNS 1.0 code; because of the lack of some fission product neutron cross-sections from its library, it was necessary to generate them using NJOY99 code. In the MONTEBURNS runs, all the fission products are considered as "important" and they are the same as those considered in the CP_2D computations. The k-infinity values have the same behavior with the void fractions and burn-up points (Fig.14).

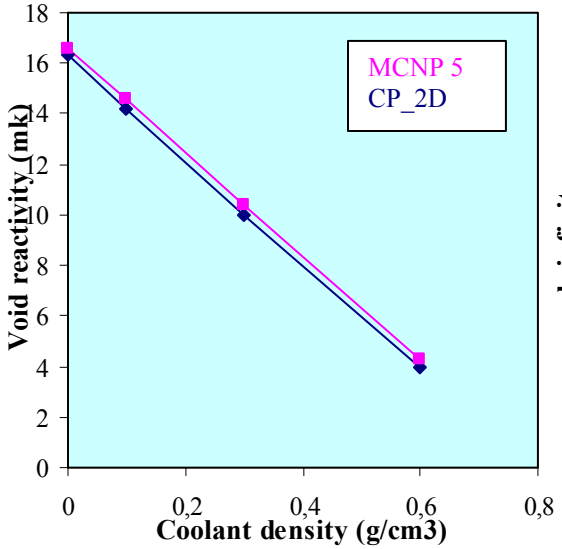

Figure 13. CANDU standard - fresh fuel

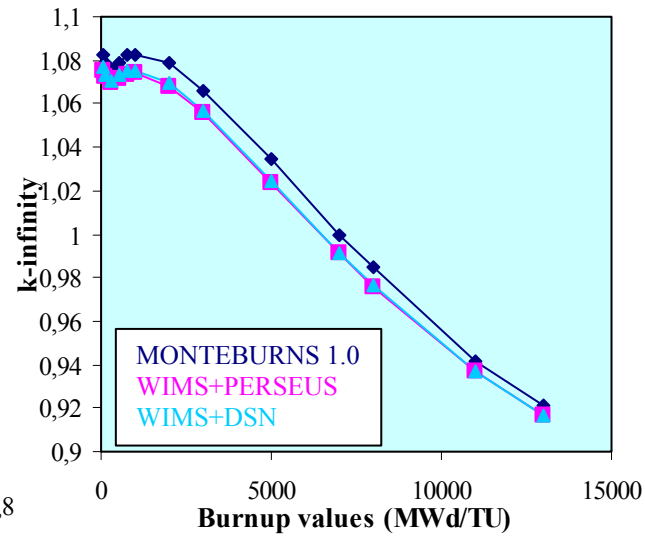

Figure 14 k-infinity as a function of burn-up

In the Monte Carlo simulations performed for CANDU- SEU (two fuel type element sizes) a two-stratified model [7] of the loss of coolant accident was considered (Fig. 12). Because of the horizontally positioning of the bundles in the pressure tube, a separation of the coolant into a liquid and a vapor phase could occur during LOC.

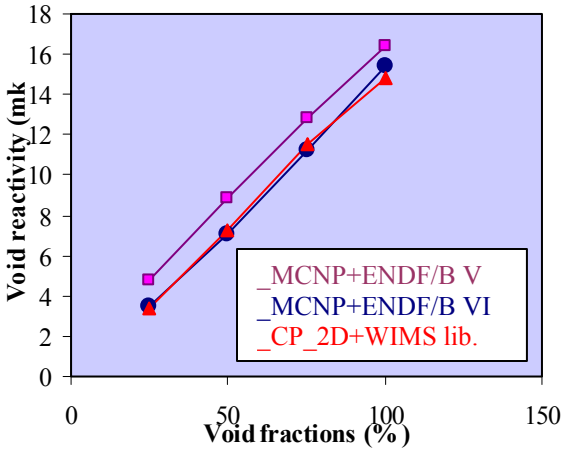

Figure 15. CANDU - SEU - fresh fuel

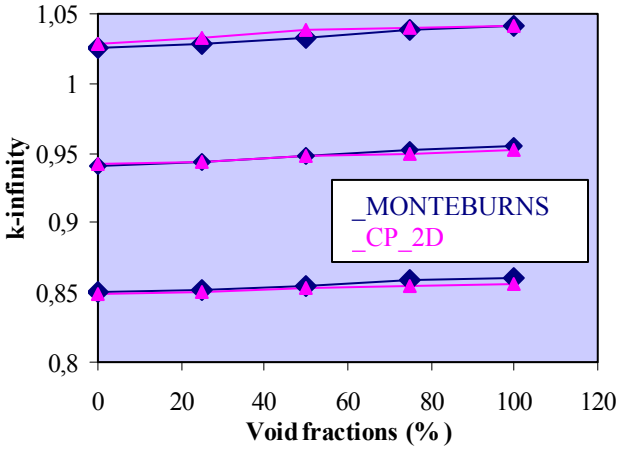

Figure 16. CANDU-SEU - burn-up results

MCNP 5 computations using the KCODE option are performed for fresh fuel and various void fractions, as well as for both ENDF/B V and ENDF/B VI libraries. The difference in the void reactivity values (MCNP 5 vs. CP_2D) is almost constant and is up to 7%; the two different libraries could also induce a difference of 2 mk (Fig. 15).

MONTEBURNS 1.0 is used in the burn-up computations; 65 new isotope cross-sections were implemented in the code library. The results carried out show the same behavior of the k-infinity values with burn-up points and void fractions as for CP_2D runs (Fig. 16). The differences (increasing with burn-up) are mainly due to the method of treating the fission products in the above codes; in MONTEBURNS runs all the fission products are considered as being "important" while in CP_2D computations only 35 of them are treated explicitly and the remainders are lumped in a single pseudo-product.

Additional simulations are performed using the option of lump all the fission products as a sum, but the k-infinity values obtained show an abnormal decreasing with burn-up; it seems that this option is not suitable for this type of applications.

5 ^{60}CO PRODUCTION IN CANDU TYPE REACTORS

During the work related to the replacement of the original stainless steel adjuster rods with ^{59}Co rods, MCNP 5 and MONTEBURNS 1.0 codes are used in order to accomplish the requirements concerning the criticality equivalence, to evaluate the activity and the heating of cobalt rods after one year irradiation, and to estimate the dose at the surface of the device designed for the removal and transportation of cobalt adjuster assemblies. The neutronic equivalence results in identical reactivity values and the same effects on the spatial distribution of the neutron flux for both stainless steel and cobalt adjuster rods.

As a result, MCNP 5 criticality computations for both adjuster types are performed in order to estimate the needed number of cobalt pellets which are supposed to be irradiated in vertical tubes (their axes are symmetrically placed on a cylindrical surface), as well as their spatial arrangement. The systems modeled in the MCNP5 code input consist in eight standard CANDU cells and the corresponding segment of the adjuster type which has to be analyzed (Fig. 17). In the calculations performed a Watt spectrum was used as starting source of neutrons with a uniform volume distribution in all the fuel pins; the material temperatures were also considered.

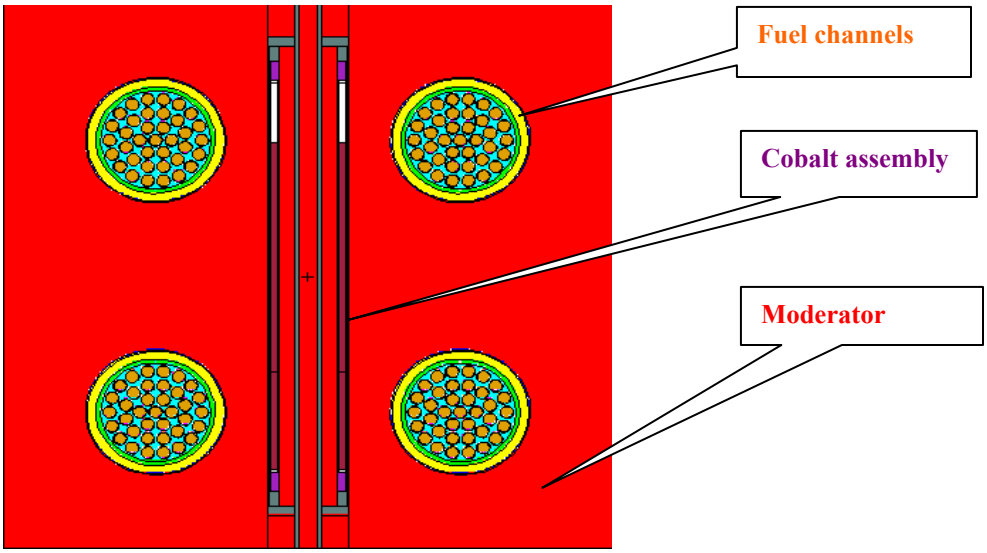

Figure 17. MCNP 5 view of the system model

All the Monte Carlo runs were performed using the KCODE capability of the MCNP5 code with the following options: a total of 8000 cycles to be done, 80 inactive cycles, and a number of 4000 source histories per cycle. In Tab. II are presented the absolute values for the local reactivity (defined as $1000*(|1/k_{ref} - 1/k_i|)$ for the stainless steel adjuster rods and for the corresponding Co adjuster assemblies. k_{ref} represents the "reference" k-infinity value (without adjuster segment inserted) and k_i are the values obtained for each adjuster type.

Table II. Adjuster reactivity values

Adjuster segment type	Stainless steel	Fresh cobalt
A-outer	24.492	25.583
A-inner	29.387	30.490
B	44.295	45.337
C-outer	17.779	18.052
C-inner	39.119	40.384
D	26.096	27.325

The next step is the computations of cobalt rod activities after one year of in-core irradiation using the MONTEBURNS1.0 code and the ORIGEN2.1 as stand-alone code. The latter is used in order to obtain information about the activities of Co^{60} and Co^{60m} isotopes, which are of interest for safety evaluations and which neutron cross-sections are missing from MCNP library. Additional computational steps are needed in order to accommodate ORIGEN for burn up evaluations when the flux-spectrum is different from that one in the fuel region.

The ORIGEN2.1 one-group cross-sections for radiative capture reactions of cobalt isotopes have been replaced with the values obtained by weighting the corresponding reaction rates with the flux-spectrum calculated for each type of the Co adjusters using MCNP5 code. A detailed energy grid of 30 points in the range 0.0 eV – 20 MeV was used in the simulation in order to obtain an accurate description of the flux in the thermal, epithermal and fast range. In the following, the ORIGEN2.1 runs were performed using the IRF option (irradiation for a single interval with the neutron flux specified - the flux values in each Co adjuster and for each irradiation step were supplied based on prior MONTEBURNS code runs). The next step consisting in the evaluation of the dose rate at the surface of the flask was performed using the MCNP5 code; a detailed description of the device (Fig. 18 - actual dimensions and material composition) is considered.

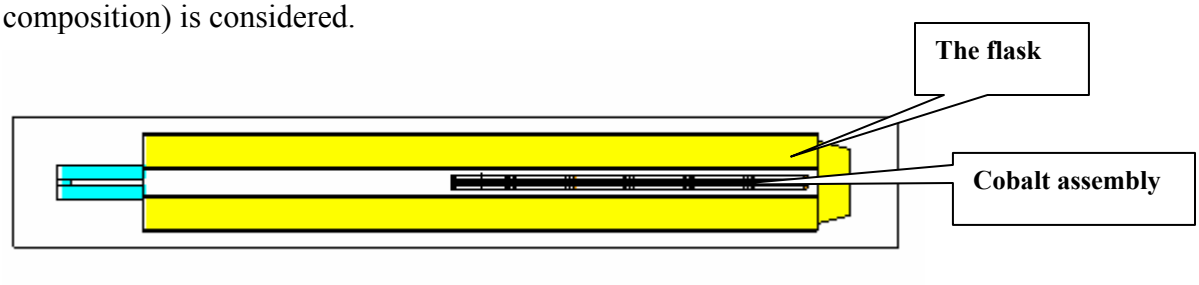

Figure 18. Cobalt adjuster transport device (the flask)

The source of the photons has a uniform volume distribution in all the cobalt regions of the adjuster with the discrete energy distribution specific to ^{60}Co isotope; the photon flux-to-dose rate conversion factors from MCNP5 library were used in the dose rate estimation. The surface contact dose rate for the most active cobalt adjuster type B evaluated at the top of the flask (where additional shielding is provided, and an operator could handle the device for a short period of time and) is of 41 mRem/h, value considered as being acceptable.

6 CONCLUSIONS

The agreement between results obtained in the work presented above and experimental measurements or other codes computations show that the Monte Carlo codes represent the best option. Moreover, there are many cases where other methods fail or are inappropriate.

Therefore, due to their versatility and capabilities, the Monte Carlo codes are considered as representing the most suitable tools in solving the complex, three-dimensional problems related to TRIGA and CANDU reactor types.

7 ACKNOWLEDGMENTS

I would like to express my special gratitude to Dr. R.J. Ellis, the official representative of the Oak Ridge National Laboratory Sister Laboratory Program, for his permanent interest, assistance and actions on behalf of Institute for Nuclear Research – Pitesti, Romania.

I would also like to thank DOE and its Office of International Safeguards' Sister Laboratory Program and RSICC (Radiation Safety Information Computational Center, ORNL) officials for their strong and constant support offered to our institute.

8 REFERENCES

[1] X-5 Monte Carlo Team, MCNP – A General Monte Carlo N-Particle Transport Code, Version 5, (2003).

[2] SCALE: A Modular Code System for Performing Standardized Computer Analyses for Licensing Evaluation, Vols. I-III, NUREG/CR-0200, Rev. 4 (ORNL/NUREG/CSD-2/R4), April 1995. Available form Radiation Shielding Information Center at Oak Ridge National Laboratory as CCC-545: RSICC (ORNL) Computer Code Collection, SCALE 4.4a, RSICC Code Package, CCC-545, (2000)

[3] RSICC (ORNL) Computer Code Collection, Monte Carlo N-Particle Transport Code System for Multiparticle and High Energy Applications, CCC-705, (2000).

[4] RSICC (ORNL) Computer Code Collection, MONTEBURNS 1.0: An Automated, Multi-Step Monte Carlo Burnup Code System, RSICC Code Package, PSR-455

[5] RSICC (ORNL) Computer Code Collection, ORIGEN-ARP 2.00, Isotope Generation and Depletion Code System-Matrix Exponential Method with GUI and Graphics Capability, CCC-702, (2002).

[6] RSICC (ORNL) Computer Code Collection, ORIGEN2.1: Isotope Generation and Depletion Code-Matrix Exponential Method, CCC-371.

[7] M. Constantin, D. Gugiu, V. Balaceanu, "Void reactivity and pin power calculation for a CANDU cell using the SEU-43 fuel bundle", *Annals of Nuclear Energy*, **30**, pp.301-316 (2003).

[8] T. Angelescu, et al., "A neutron irradiation facility for damage studies", *Nucl. Instr. & Meth.in Physics Research*, **A 345**, pp.303-307 (1994).

[9] N.P. Kocherov, P.K. McLaughlin, *The International Reactor Dosimetry File (IRDF-90 Version 2)*, IAEA-NDS-141 (1993).

[10] C. Roth, et al., "The ΣΣ Secondary Intermediate-Energy Standard Neutron Field Development at the Romania TRIGA Reactor", *Nucl. Instr.&Meth. in Physics Research*, **A522,** pp.462-469 (2004).